Influence of Strains on Paramagnetic-Resonance Spectrum for Strongly Coupled Ions—Application to V^{3+} in MgO

R. Buisson and A. Nahmani
Laboratoire de Spectrométrie Physique, Université Scientifique & Médicale de Grenoble, Cedex 53, 38-Grenoble-Gare, France*
(Received 9 March 1972)

We develop a Monte Carlo method to study the influence of static random strains on EPR and acoustic-paramagnetic-resonance (APR) spectra. The method consists of calculating the line shape using random numbers which represent the random strains. We have applied this method to the particular case of a $S=1$ system in cubic symmetry in the presence of Γ_{3g}-type strains. The important parameter is the product of the strain-ion coupling coefficient and the width of the distribution function of the strains. When this parameter is small compared to the Zeeman term, we find the known results obtained using perturbation theory. When this parameter is of the order of the Zeeman term, the line shape is profoundly modified and the spectrum has great similarity to an axial spectrum. The comparison between calculated and experimental spectra obtained with MgO:V^{3+} confirms the previously proposed interpretation. The strain-ion coupling coefficient is deduced from this comparison. We also discuss the possibility of deducing the Jahn-Teller energy and covalency from our recent experimental results interpreted within the model developed here. The values obtained show that Jahn-Teller coupling is only slightly greater than spin-orbit coupling. Thus, the MgO:V^{3+} system appears to be near the limit where the Jahn-Teller effect is stabilized by spin-orbit coupling.

I. INTRODUCTION

It is well known that random static strains which exist even in good crystals are frequently the cause of line broadening in electron paramagnetic resonance (EPR) and acoustic paramagnetic resonance (APR). Quantitative calculations of their effect have been made for two typical situations. In one, the ions are relatively weakly coupled to the lattice as compared to the Zeeman interaction, so that perturbation theory can be applied.[1-3] Stoneham has given a review of the subject.[4] The other situation concerns strongly coupled ions and particularly some ions subject to the Jahn-Teller effect. In the case of the $SrCl_2:La^{2+}$ and $CaF_2:Sc^{2+}$ systems,[5-7] and more recently in the case of the $MgO:Cr^{2+}$ system,[8,9] the observed spectra have been explained on the basis of the strain effect exceeding the Zeeman effect. In the first situation, the spectrum has the average symmetry of the site. In the second, the experimental method of observation can "select" some of the ions which are in particular distorted sites. The resulting spectrum no longer has the average symmetry of the site and it can be strain dependent.

In a previous paper on the $MgO:Fe^{2+}$ system,[10] we made an exact calculation, instead of using perturbation theory, for a particular magnetic field orientation. This calculation showed that the center of the $\Delta M=1$ line is strain dependent. The purpose of this paper is to study, using a new approach, the more general problem of a triplet state in cubic symmetry for which the strain and Zeeman interactions are of the same order of magnitude. This is, indeed, the case for V^{3+} in MgO and we show that the interpretation we have proposed[11] is correct. In particular, our calculations describe very well the shape of the spectrum and its angular dependence, while the work of Ray[12] does not. We also obtain some results which confirm qualitatively Ham's interpretation of the spectrum of Cr^{2+} in MgO.[9] (See note added in proof.)

In Sec. II we describe the method used which has some features in common with a Monte Carlo calculation. The general results we obtain are given in Sec. III. We then compare the theoretical and the experimental spectra for the V^{3+} ion in MgO and we deduce the magnitude of the strain-ion coupling. In Sec. IV, we discuss the values of the physical constants, such as Jahn-Teller coupling and covalency, deduced from our recent experimental results.

II. DESCRIPTION OF METHOD

The general Hamiltonian for a triplet state in cubic symmetry and in the presence of strains and magnetic field can be written

$$\mathcal{H}=g\mu_B(\vec{H}_0\cdot\vec{S})+\tfrac{1}{2}G_{11}\left([3S_z^2-S(S+1)]\,e(\Gamma_{3g},\theta)+\tfrac{1}{2}\sqrt{3}\,(S_+^2+S_-^2)\,e(\Gamma_{3g},\epsilon)\right)$$

$$+\frac{G_{44}}{\sqrt{5}}\left((S_+S_z+S_zS_+)e(\Gamma_{5g},1)-\frac{1}{\sqrt{2}}(S_+^2-S_-^2)e(\Gamma_{5g},0)+(S_-S_z+S_zS_-)e(\Gamma_{5g},-1)\right), \quad (1)$$

where the strains $e(\Gamma_\alpha,\beta)$ have the usual definitions[13,14]:

$$\begin{aligned} e(\Gamma_{1g}) &= (1/\sqrt{2})(e_{xx}+e_{yy}+e_{zz}) \ , \\ e(\Gamma_{3g},\theta) &= \tfrac{1}{2}(2e_{zz}-e_{xx}-e_{yy}) \ , \\ e(\Gamma_{3g},\epsilon) &= \tfrac{1}{2}\sqrt{3}(e_{xx}-e_{yy}) \ , \\ e(\Gamma_{5g},0) &= i\sqrt{3}e_{xy} \ , \\ e(\Gamma_{5g},\pm 1) &= \mp i\sqrt{\tfrac{3}{2}}(e_{yz}\pm ie_{xz}) \ . \end{aligned} \quad (2)$$

In the Hamiltonian (1), the g value takes into account the spin-orbit coupling, the Ham reduction, and possibly the effect of covalency. G_{11} and G_{44} are the conventional coefficients, often called the spin-phonon coefficients, which characterize the coupling of the ion with the distortions of the cubic site. The strains vary from site to site and we shall consider that they are random quantities with a Gaussian distribution. This choice is one of convenience, but we think that other choices would not greatly modify the results. This point will be discussed in Sec. III.

We consider the frequently encountered case for which the coupling with the Γ_{3g} strains is dominant. This hypothesis will be justified *a posteriori*, for the system V^{3+}:MgO, by the good agreement between theoretical and experimental spectra. Also, we limit most of the calculation to the problem of an ion without hyperfine coupling. Again, these points will be discussed in Sec. III.

The successive steps of the method are the following: (i) Pairs of random numbers $[e(\Gamma_{3g},\theta), e(\Gamma_{3g},\epsilon)]$ are numerically generated, i.e., the distortion of a site for an ion is defined; (ii) the values of the magnetic field for which two levels of the ion are separated by the quantum $\hbar\omega_0$ are deduced; (iii) the eigenstates are determined; (iv) the transition probability between the two states is then calculated.

In order to obtain more general results, we write the Hamiltonian (1) in the reduced form

$$\begin{vmatrix} a+h & k & c \\ k^* & -2a & k \\ c & k^* & a-h \end{vmatrix} \ , \quad (3)$$

where

$$\begin{aligned} h &= \lambda\cos\theta \ , & k &= \lambda\sin\theta\, e^{-i\phi}/\sqrt{2} \ , \\ \lambda &= g\mu_B H_0/\hbar\omega_0 \ , & a &= \alpha\sqrt{6}X \ , \\ c &= 3\alpha\sqrt{2}Y \ , & \alpha &= G_{11}/4\hbar\omega_0 \ , \\ X &= \sqrt{\tfrac{2}{3}}e(\Gamma_{3g},\theta) \ , & Y &= \sqrt{\tfrac{2}{3}}e(\Gamma_{3g},\epsilon) \ , \end{aligned} \quad (4)$$

the magnetic field orientation being defined by the polar angles (θ,ϕ). The variables X and Y have a Gaussian distribution of width 2δ. Two parameters, α and δ, appear, but the result depends only on their product $\alpha\delta$. We choose arbitrarily $\alpha=\frac{1}{80}$, a value which corresponds to the case of Fe^{2+} in MgO when the width δ is expressed in terms of 10^{-5} units strain. Thus, the width Δ of the distribution for the strains e_{ii} themselves has a numerical value given by $\Delta=\delta\times10^{-5}$ and the product $\alpha\delta$ is $\alpha\delta=G_{11}\Delta/4\hbar\omega_0$. However, we stress that with the choice of the reduced variables, the important parameter is the product $\alpha\delta$ (or $G_{11}\Delta$) and that a variation in δ will mean as well a variation in the ion-strain coupling or a variation in the width of the strain distribution.

For each set of calculation, we fix the values of δ,θ,ϕ. Once the pair (X,Y) is defined, the eigenvalues of (3) are the roots of a cubic equation of the form

$$x^3+xp(\lambda)+q(\lambda)=0 \ , \quad (5)$$

where p and q depend only on λ. The resonance can occur if two of these roots have a difference of 1. It is easy to show that this is true if λ is a root of

$$1+6p+9p^2+4p^3+27q^2=0 \ . \quad (6)$$

This equation is of third degree with respect to λ^2 and has 0, 1, 2, or 3 positive roots (negative roots correspond to opposite magnetic field orientation and are not considered). Putting these values in (3), we calculate the eigenvectors and from them the transition probability. For this last calculation, we use the Hamiltonians

$$\mathcal{H}_1=g\mu_B(\vec{H}_1\cdot\vec{S})\cos\omega t \quad (7)$$

for EPR transitions and

$$\mathcal{H}_1=\tfrac{1}{8}G_{11}e_{xx}\{3(S_+^2+S_-^2)-2[3S_z^2-S(S+1)]\}\cos\omega t \quad (8)$$

for APR transitions induced by longitudinal acoustic waves propagating in the x direction.

Calculations have been made with an IBM 360-65 computer. The Gaussian numbers were generated by a method given in Appendix B. Various histograms were made to test the Gaussian character of the numbers generated. The shape of the surface of the probability density $p(X,Y)$ was monitored and no correlation between two successive numbers was observed. Most of the results were obtained with only 1000 pairs (X,Y). For a given magnetic field orientation and a given value δ, the calculation takes from a few seconds to 1 min.

As shown in Appendix A, the line shape can be obtained by the evaluation of an integral. In order

to test the validity of the numerical method, we have compared the obtained results with the theoretical line shape for two cases where the problem is analytically solvable. The first case corresponds to the EPR absorption with $\vec{H}_0$ along [001] and the radio-frequency field $\vec{H}_1$ along [100]. The result is[15]

$$I(\lambda) = A\lambda \exp\left(-\frac{1+\lambda^2}{108\,\alpha^2\delta^2}\right)\int_{-\infty}^{+\infty} dY\, \frac{e^{-2Y^2/36^2}}{(\lambda^2+18\,\alpha^2 Y^2)^{1/2}} \times\left[\exp\left(\frac{(\lambda^2+18\alpha^2Y^2)^{1/2}}{54\alpha^2\delta^2}\right) + \exp\left(-\frac{(\lambda^2+18\alpha^2Y^2)^{1/2}}{54\alpha^2\delta^2}\right)\right], \quad (9)$$

where A is a constant. This integral is easily evaluated by numerical computation. The second case corresponds to acoustic resonance with longitudinal waves propagating along [100] and with $\vec{H}_0$ along [001]. The line shape is then

$$I(\lambda) = B\,\frac{\lambda^3}{(1-4\lambda^2)^{1/2}}\exp\left(-\frac{1-4\lambda^2}{144\alpha^2\delta^2}\right), \quad (10)$$

where B is a constant. This last equation shows the existence of a singularity at $\lambda = \frac{1}{2}$. This singularity comes from the fact that the line due to each ion has been supposed to be infinitely narrow. Apart from the nearest values of λ, this singularity has no effect. Figures 1 and 2 show the comparison of the theoretical results (9) and (10) with the numerical computation. The agreement is very good. To make clearer, in what follows, the comparison between experimental and calculated spectra, we present "smoothed" histograms obtained as illustrated in Fig. 3.

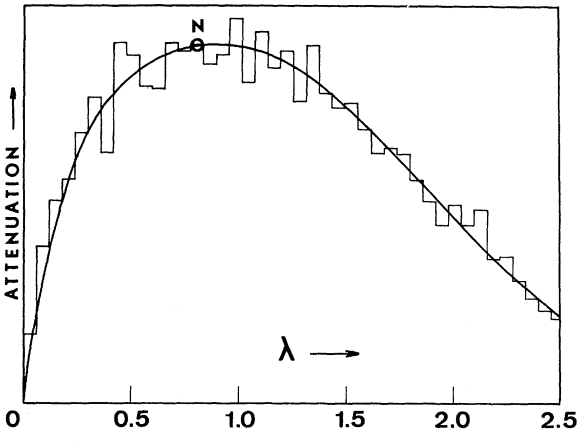

FIG. 1. EPR line shape with $\vec{H}_0$ along [001], $\vec{H}_1$ along [100], and $\delta = 10$. The histogram is the result of Monte Carlo calculation made with 5000 pairs (X, Y). The curve is drawn from Eq. (9) normalized at point N.

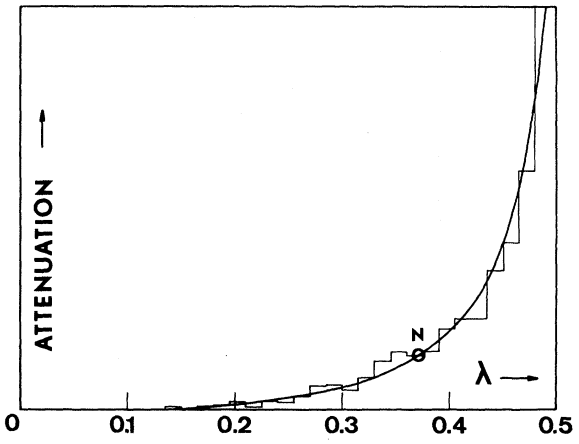

FIG. 2. APR line shape with $\vec{H}_0$ along [001], $\vec{k}$ along [100], and $\delta = 10$. The histogram is the result of Monte Carlo calculation made with 1000 pairs (X, Y). The curve represents the analytical result given by Eq. (10) after normalization at point N.

III. RESULTS

A. General Results

We have determined the APR line shape for the particular situation described in Sec. II, i.e., no hyperfine coupling, only the Γ_{3g} strains are active, the transitions are induced by the Hamiltonian (8). The value of δ is very important since it affects the general aspects of the spectrum. When δ is small we get the same results as those obtained by perturbation calculation. This is another test of the method.

When δ is such that $4\alpha\delta \sim 1$, i.e., $G_{11}\Delta \sim \hbar\omega_0$, the spectrum is anisotropic as shown in the upper part of Figs. 4 and 5. The curves correspond to

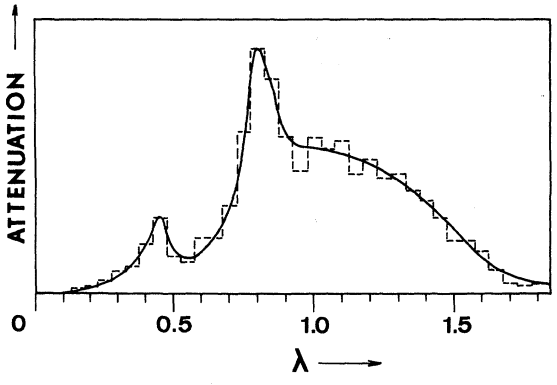

FIG. 3. Typical histogram obtained by Monte Carlo calculation and its associated "smoothed histogram." This result is obtained with 1000 pairs (X, Y), $\delta = 10$, $\vec{k}$ along [100], and with an orientation of $\vec{H}_0$ defined by the polar angles $\theta = 40°$, $\phi = 0°$.

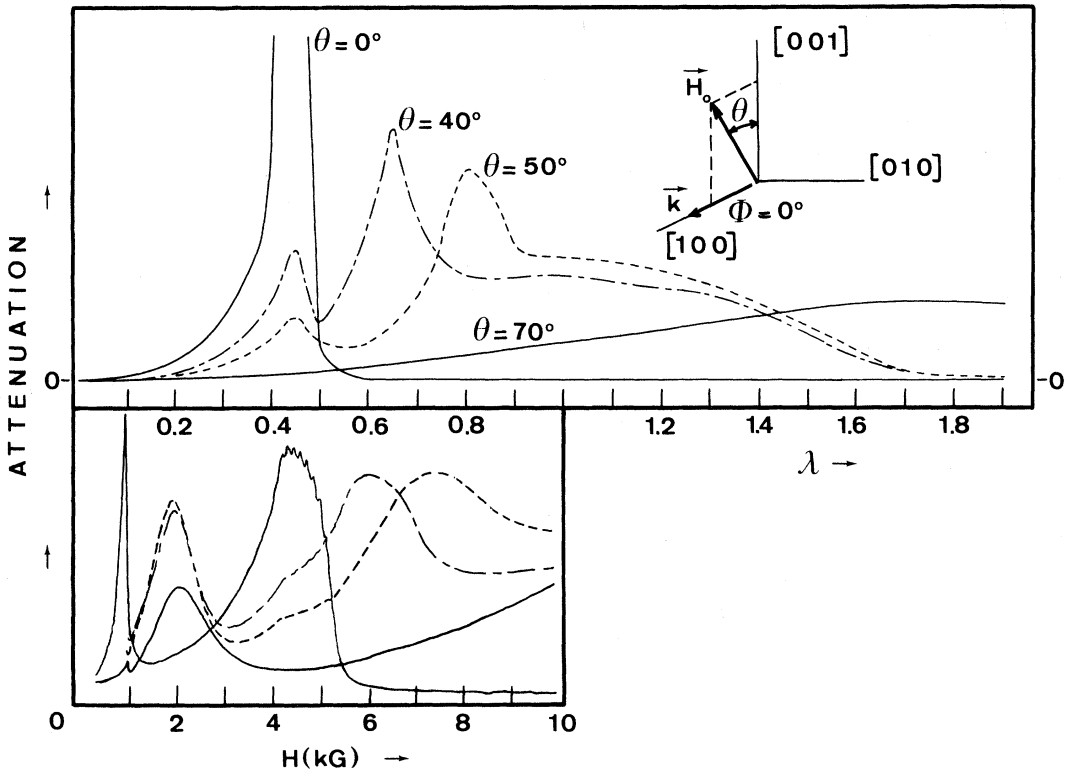

FIG. 4. Angular variation of the APR spectrum. The orientations of $\vec{H}_0$ and $\vec{k}$ are indicated. The upper curves are smoothed histograms obtained by Monte Carlo calculation with 1000 pairs (X, Y) and $\delta = 10$. The lower curves are the experimental results from Ref. 11. (Note that theoretical curves do not take into account the hyperfine interaction.)

the case $\delta = 10$, i.e., $G_{11}\Delta = \frac{1}{2}\hbar\omega_0$. An important point is that this behavior results from the mixing of the states and not from the fact that only the ions which are in tetragonally distorted sites give a contribution to the spectrum. As we have proposed,[11] transitions of the $\Delta m = 1$ type contribute strongly to the spectrum. This is proved by the curves corresponding to ($\phi = 0$, $\theta = 40°$) and ($\phi = 0$, $\theta = 50°$) for which the $\Delta m = 1$ line appears. With other orientations, however, the spectrum is more involved and the word "line" does not have a clear meaning. The method used here can give a good illustration of the situation. We have looked at the values of the numbers X and Y for the ions which contribute to the line near a maximum of the acoustic attenuation. Figure 6 gives the result for $\vec{H}_0 \| [011]$, i.e., $\phi = 90°$ and $\theta = 45°$. In this figure, a point represents an ion in a distorted site, the distortion being defined by X and Y, with energy levels such that a transition occurs for a value of λ such that $0.70 \leq \lambda \leq 0.75$. It is clear that these ions are in orthorhombic and not tetragonal symmetry. In addition, the examination of their energy levels shows that the transition is of $\Delta m = 1$ type. All these observations confirm the interpretation we had proposed to explain our experimental spectra, some of which being drawn in the lower part of Figs. 4 and 5. Both V^{3+} and Fe^{2+} spectra are visible. The latter corresponds to a smaller value for δ because the strain-ion coupling is smaller; the anisotropy is manifested mostly in the linewidth. For the spectrum of V^{3+}, even with the presence of hyperfine structure the essential behavior is explained by the theoretical curves.

When δ is increased, the spectrum is again modified. The curves of Fig. 7 are obtained with $\delta = 100$, i.e., $G_{11}\Delta = 5\hbar\omega_0$. The spectrum is also anisotropic but the line shapes are very different, indicating the $\Delta m = 2$ nature of the transitions. In addition, fewer ions contribute to the lines because distortions can be very strong, hence making impossible the resonance condition. We observed that the maximum of the line intensity was about five times smaller with $\delta = 100$ than with $\delta = 10$. Also, the intensity is not zero outside the lines and this would result, in an experiment, in a smaller signal-to-noise ratio. This decrease in the line intensity leads us to use 5000 pairs (X, Y) instead of 1000 for $\delta = 10$. Again we can look at the distortion of the sites for the ions which contribute to the lines. We have plotted in Fig. 8 the values of (X, Y) for

those ions when $\phi = 90°$, $\theta = 22°30'$, an orientation for which two lines exist (see Fig. 7). One can see that the low-field line is due to ions which are in tetragonal sites, with the y axis being the symmetry axis, and that the high-field line is also due to ions which are in tetragonal sites but with the z axis being the symmetry axis. Thus, only a fraction of the ions are observed and, even with a strain distribution centered around zero, the spectrum shows an axial symmetry. These results are in agreement with Ham's explanation of the spectrum of Cr^{2+} in MgO.[9] We can point out that although the symmetry is axial as for systems which show a static Jahn-Teller effect, the situation is in fact very different. In the static case, the Jahn-Teller coupling dramatizes the effect of random static strains and the final distortion has a value unrelated to the value of the original strain, the symmetry being, however, the same. In addition, *all* the ions are in one of the three distorted sites (of course, only if the coupling with the Γ_{5g} strains is neglected). On the other hand, in the systems studied here only some of the ions are observed and the intensity of the lines diminishes as the strength of the strains increases.

B. Application to V^{3+} in MgO. An Estimate of Strain-Ion Coupling

After obtaining qualitative agreement between experimental and theoretical spectra, we can go further and try to deduce the value of the strain-ion coupling coefficient G_{11}. However, the hyperfine structure introduces complications. We can overcome these complications for two particular cases. The first concerns the orientation for which $\vec{H}_0$ is parallel to [001]. If there we treat the hyperfine strucure as a perturbation, the problem is analytically solvable and the line shape is readily deduced. The second interesting situation corresponds to the case where strain broadening is very much stronger than the hyperfine interaction. We now discuss these two situations.

When $\vec{H}_0$ is along [001], the Hamiltonian (3) is easily solved. Let E_i and $|i\rangle$ be the eigenvalues and the eigenvectors. The eigenvector $|i\rangle$ can be written

$$|i\rangle = l_i|1\rangle + m_i|0\rangle + n_i|-1\rangle \ .$$

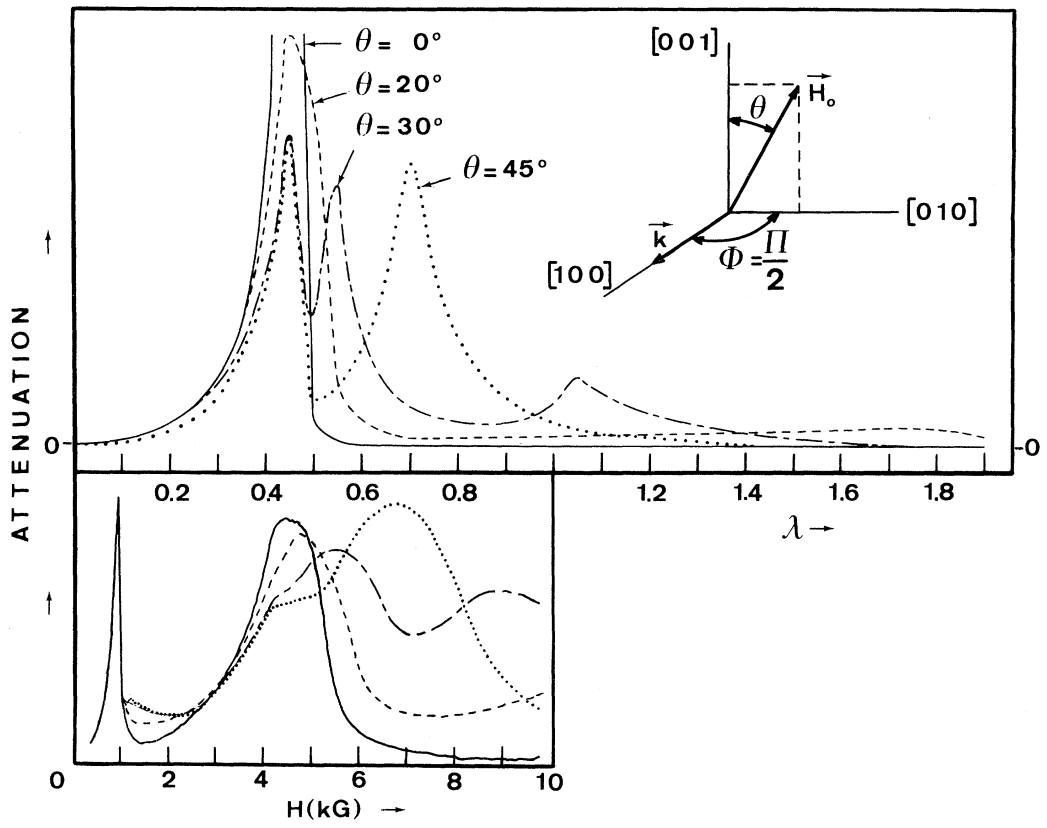

FIG. 5. Angular variation of the APR spectrum. The orientations of $\vec{H}_0$ and $\vec{k}$ are indicated. The upper curves are smoothed histograms obtained by Monte Carlo calculation with 1000 pairs (X, Y) and $\delta = 10$. The lower curves are the experimental results from Ref. 11. (Note that theoretical curves do not take into account the hyperfine interaction.)

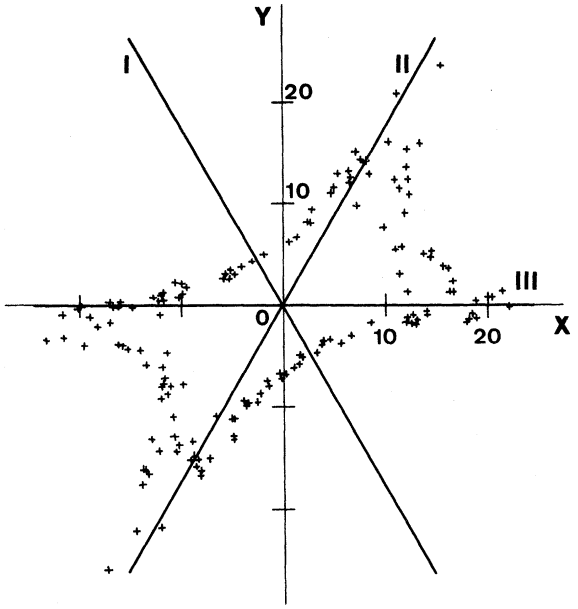

FIG. 6. APR resonance with $\delta = 10$, $\vec{k}$ along [100], $\theta = 45°$, and $\phi = 90°$ (see Fig. 5). The coordinates of each point are the reduced strains of the ions which contribute to the part of the line for $0.70 \leq \lambda < 0.75$, i.e., near the high-field maximum. The straight lines I, II, and III correspond to tetragonal distortion of axis x, y, z.

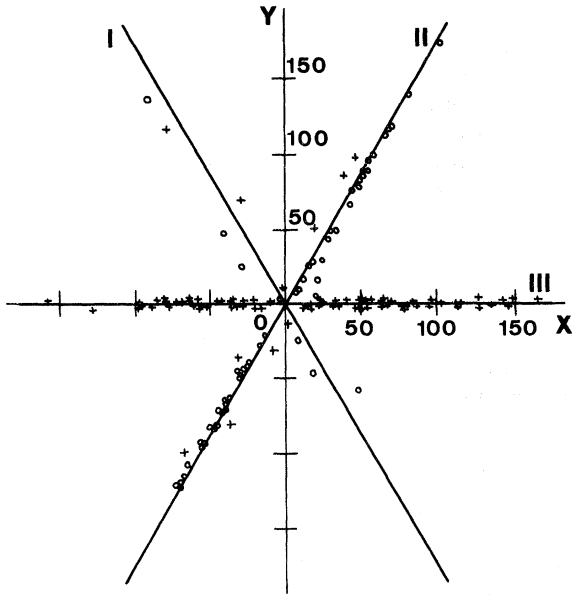

FIG. 8. APR resonance with $\delta = 100$, $\vec{k}$ along [100], $\theta = 22° 30'$, $\phi = 90°$ (see Fig. 7). The coordinates of the points + are the reduced strains of the ions which contribute to the part of the line for $0.5 \leq \lambda < 0.55$; the coordinates of the points O (open circle) are the reduced strains of the ions which contribute to the part of the line for $1.30 \leq \lambda < 1.35$. The straight lines I, II, III correspond to tetragonal distorsion of axis x, y, z.

By a well-known method,[16] one can show that, inside the manifold $|i\rangle$, the hyperfine structure is described by

$$A_{\text{eff}}^{(i)} I_Z(i) \ ,$$

where $Z^{(i)}$ is a new quantum axis defined by the direction cosines

$$\frac{\alpha_i}{(\alpha_i^2+\beta_i^2+\gamma_i^2)^{1/2}} \ , \quad \frac{\beta_i}{(\alpha_i^2+\beta_i^2+\gamma_i^2)^{1/2}} \ ,$$

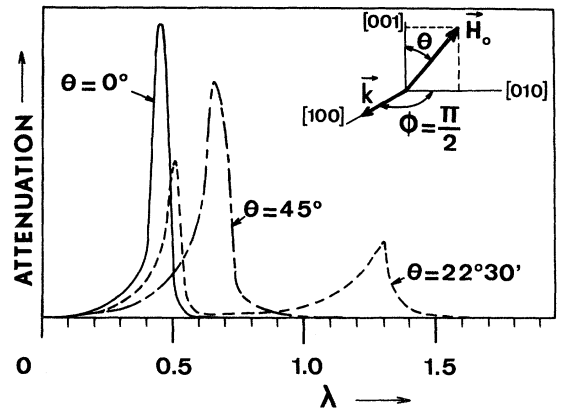

FIG. 7. Angular variation of the APR spectrum. The orientations of $\vec{H}_0$ and $\vec{k}$ are indicated. The curves are smoothed histograms obtained by Monte Carlo calculation with 5000 pairs (X, Y) and $\delta = 100$.

$$\frac{\gamma_i}{(\alpha_i^2+\beta_i^2+\gamma_i^2)^{1/2}} \ ,$$

with

$$\alpha_i = \langle i|S_x|i\rangle \ , \quad \beta_i = \langle i|S_y|i\rangle \ , \quad \gamma_i = \langle i|S_z|i\rangle \ ,$$

and where

$$A_{\text{eff}}^{(i)} = A(\alpha_i^2+\beta_i^2+\gamma_i^2)^{1/2} \ ,$$

A being the usual hyperfine parameter.

When $\vec{H}_0$ is along [001], the eigenvalues are

$$E_0 = -2a, \quad E_\pm = a \pm (\lambda^2+c^2)^{1/2} \ ,$$

and the corresponding values for A_{eff} are, in reduced form,

$$A_0' = A_{\text{eff}}^{(0)}/\hbar\omega = 0 \ ,$$

$$A_\pm' = A_{\text{eff}}^{(\pm)}/\hbar\omega = \lambda A/\hbar\omega(\lambda^2+c^2)^{1/2} = A' \ ,$$

with opposite directions for the $Z^{(+)}$ and $Z^{(-)}$ axis. The line shape is then, for the transitions $\Delta M_I = 0$,

$$I(\lambda) = \sum_{M=-7/2}^{+7/2} I(\lambda, M) \ ,$$

with

$$I(\lambda, M) = \frac{3\lambda^2[(4\lambda+2MA')(\lambda^2+c_1^2)^{1/2}-\lambda]}{2\delta\sqrt{\pi}\alpha c_1(\lambda^2+c_1^2)[1-4(\lambda^2+c_1^2)^{1/2}]} \ e^{-\gamma_1^2/2\delta^2} \ , \tag{11}$$

where c_1 is defined by

$$c_1^2 + \lambda^2 = \tfrac{1}{8}[1 - 8MA'\lambda + (1 - 16MA'\lambda)^{1/2}]$$

and

$$Y_1 = c_1/3\alpha\sqrt{2} \ .$$

Equation (11) has singularities for $\lambda = \frac{1}{2} + MA'$ analogous to that of Eq. (10) but we can try to fit the theoretical line shape with the experiments for values of λ not too near the critical values. Figure 9 shows that no value of δ is convenient. This disagreement could arise from the use of perturbation theory, because this approximation is not correct for some ions. However, we think the number of these ions is too small to affect significantly the line shape. Another reason could be the choice of the Gaussian shape for the distribution of the random strains. Although a Lorentzian shape does not give a better agreement, other shapes are plausible. Finally, the disagreement could also be due to the Γ_{5g} strains which have been ignored in the calculation. We have made some attempts to see their influence. Besides the necessity to work with three additional random variables, the omission of the hyperfine interaction makes the comparison with experiments difficult. This problem is now under study.

We consider now the case where $\vec{H}_0$ is far from a $\langle 100 \rangle$ axis. The lines become very broad in the region of $\lambda = 1$ and the effect of hyperfine interaction is masked. We have calculated the shape of the lines for various values of δ when $\theta = 40°$ and $\phi = 0°$ and when $\theta = 40°$ and $\phi = 90°$. Part of the results are given in Fig. 10. They show that the spectrum is strongly strain dependent, as experimentally observed, for instance, with Cr^{2+} in MgO.[17] But these results can also be used to deduce a value for δ. The curves of Fig. 10 show, for instance, that the ratio of the intensity at $\lambda = 1$ to the intensity at the maximum near $\lambda = 0.75$ is

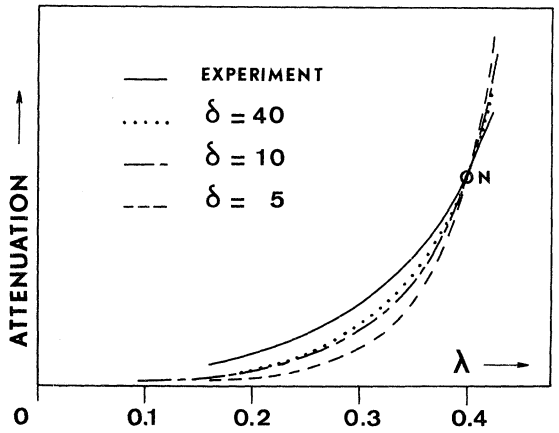

FIG. 9. Comparison of the APR experimental line shape with theoretical results for $\vec{H}_0$ along [001], and $\vec{k}$ along [100]. N is the point of normalization.

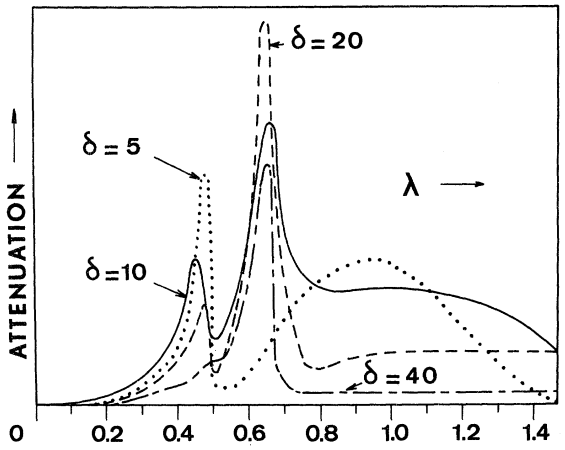

FIG. 10. APR spectrum for various values of the parameter δ. $\vec{k}$ is along [100] and the orientation of $\vec{H}$ is defined by $\theta = 40°$, $\phi = 0°$. The Monte Carlo calculation was made with 5000 pairs (X, Y) for $\delta = 40$ and $\delta = 20$ and with 1000 pairs for $\delta = 10$ and $\delta = 5$. (The curves are not drawn at the same scale.)

very sensitive to the value of δ. Comparison with the experimental spectrum given in Fig. 4 leads to the value $\delta \sim 10$. If we suppose the same distribution for the strains in the vicinity of V^{3+} and of Fe^{2+}, we can deduce the value of G_{11} for V^{3+} from that of Fe^{2+}. We get $G_{11} \sim 1500$ cm^{-1} per unit strain.

A value for G_{11} can be deduced from the magnitude of the acoustic attenuation. For a longitudinal wave propagating along [100] and with $\vec{H}_0$ parallel to [001], this attenuation is given by

$$\alpha = \frac{3\pi N' \omega_0^2 g(\omega) G_{11}^2}{16\rho v^3 kT} \ (\text{cm}^{-1}) \ .$$

Here, N' is the total population per cm^3 of the excited triplet in which the resonance is observed. The presence of the line shape $g(\omega)$ is a complication in the use of this formula. Fortunately, we can use the results of the preceding calculations which show that 13% of the ions contribute to the line for a range of 100 Gs about the maximum of attenuation. It is then possible to consider $g(\omega)$ as a rectangular line of width $\Delta\omega = (g\mu_B/\hbar)\Delta H$ due only to 13% of the ions. The nominal concentration for the vanadium is 10^{-4} ions. We suppose that 60% are in the trivalent state. Taking the values of $\rho = 3.58$ g/cm^3, $v = 9 \times 10^5$ cm/sec, we obtain $G_{11} = 950$ cm^{-1}. In view of the uncertainty of the concentration, this value compares well with the preceding one.

IV. ADDITIONAL COMMENTS ON SPECTRUM OF V^{3+} IN MgO

The experimental results of Brabin-Smith and Rampton[18] interpreted as an axial spectrum have been discussed elsewhere.[12,19] We wish here to

deduce new values for the physical constants from our recent experimental results[11] and within the interpretation developed here which supposes that the sites of the V^{3+} ions are, on the average, cubic. The experiments yield essentially two quantities: the g value and the splitting between the two low-lying multiplets. We begin to discuss the various mechanisms which are at the origin of the splitting of these multiplets.

A. Splitting between Two Low-Lying Multiplets

The ground term ^3F obtained from the configuration $3d^2$ of the V^{3+} ion is split by the cubic crystal field leaving a Γ_{4g} triplet as the ground state (see Fig. 11). However, term mixing is not negligible and we must write the ground state as

$$|\Gamma_{4g}\rangle = \cos\alpha\,|^3\Gamma_{4g}, te\rangle + \sin\alpha\,|^3\Gamma_{4g}, t^2\rangle \quad , \qquad (12)$$

where α is given by

$$\tan 2\alpha = (12F_2 - 60F_4)/(9F_2 - 45F_4 + 10Dq) \, ,$$

F_2 and F_4 being the usual radial integrals and Dq being the parameter which characterizes the strength of the crystal field. The notation used in (12) for the states is the conventional one: $|\Gamma_{4g}, te\rangle$ is the state belonging to the Γ_{4g} irreducible representation arising from the crystal configuration te.

We then introduce the Jahn-Teller coupling supposing it to be bigger than spin-orbit coupling. We shall discuss this point later. In view of the results obtained in Sec. III, we consider only the coupling with the Γ_{3g} modes. It is well known[20] that a manifestation of the Jahn-Teller coupling is a reduction of the first-order spin-orbit coupling. Using the notation of Ham, [20] we can write

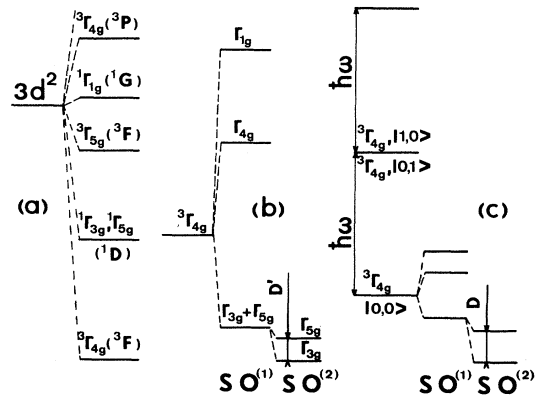

FIG. 11. Energy levels of V^{3+} ion. (a) Splitting of the configuration d^2 for the value $Dq = 1700$ cm^{-1} deduced from Sturge measurements. (b) Splitting of the ground *electronic* triplet by spin-orbit coupling at first ($SO^{(1)}$) and second order ($SO^{(2)}$). (Jahn-Teller effect is ignored.) (c) Splitting of the ground *vibronic* triplet by spin-orbit coupling at first ($SO^{(1)}$) and second order ($SO^{(2)}$).

$$\mathcal{H}_{SO}^{(1)} = \lambda_f g_L c K(\Gamma_{4g})(\vec{\mathfrak{L}} \cdot \vec{S}) \quad , \qquad (13)$$

with $\mathfrak{L} = 1$, $S = 1$, $g_L = \frac{1}{2}\sin^2\alpha - \cos^2\alpha - 2\sin\alpha\cos\alpha$, $K(\Gamma_{4g}) = e^{-3E_{JT}/2\hbar\omega}$; λ_f is the spin-orbit coupling coefficient for the free ion, E_{JT} is the Jahn-Teller energy, $\hbar\omega$ is the energy of the most active modes, and c is the covalency reduction factor. This first-order spin-orbit Hamiltonian leaves a quintuplet as a ground state and it is necessary to go to second-order effects to lift this degeneracy. As proposed by Ray, [12] we first follow Ham for the evaluation of the effect of the vibronic excited levels associated with the Γ_{4g} electronic state. The general calculation made by Ham[20] leads to the second-order effective Hamiltonian

$$\mathcal{H}_{SO}^{(2)} = K_1(\vec{\mathfrak{L}} \cdot \vec{S})^2 + K_2(\mathfrak{L}_x^2 S_x^2 + \mathfrak{L}_y^2 S_y^2 + \mathfrak{L}_z^2 S_z^2) \, ,$$

with

$$K_1 = -\frac{\lambda_f^2 g_L^2 c^2}{\hbar\omega} \exp\left(-\frac{3E_{JT}}{\hbar\omega}\right) G\left(\frac{3E_{JT}}{2\hbar\omega}\right) \, ,$$

$$K_2 = -\frac{\lambda_f^2 g_L^2 c^2}{\hbar\omega} \exp\left(-\frac{3E_{JT}}{\hbar\omega}\right) \times \left[G\left(\frac{3E_{JT}}{\hbar\omega}\right) - G\left(\frac{3E_{JT}}{2\hbar\omega}\right) \right] ,$$

where $G(x)$ is defined by

$$G(x) = \int_0^x \frac{e^u - 1}{u}\, du \quad .$$

The application to our case is straightforward and leads to a splitting of the quintuplet into a lower doublet and an excited triplet, the energy separation being

$$D = -K_2 \quad . \qquad (14)$$

However, we must look at the second-order terms due to other excited levels. For a general treatment, we ought to consider all the vibronic levels associated with all the crystal field electronic levels. This treatment would be very cumbersome. To simplify it, we shall neglect the term mixing and consider only the ground ^3F term for which $L = 3$. This term is split by the cubic field into a ground Γ_{4g} triplet, a Γ_{5g} triplet, and a Γ_{2g} singlet (see Fig. 11). As spin-orbit coupling has nonzero matrix elements only between the states of the two triplets, we do not consider the Γ_{2g} level. Ignoring for a moment the Jahn-Teller interaction, we can calculate easily the second-order effect of spin-orbit coupling inside the Γ_{4g} triplet. We find that the ground quintuplet resulting from the first-order effect is split into a lower doublet and an excited triplet, the energy separation being

$$D' = 15\lambda_f^2/2\Delta \quad , \qquad (15)$$

where Δ is the energy of the Γ_{5g} triplet. We must now introduce the Jahn-Teller interaction and dis-

cuss the possibility of the reduction of this value. The vibronic states associated with the two orbital triplets Γ_{4g} and Γ_{5g} have an electronic part identical to that which exists in the absence of the Jahn-Teller coupling and a vibrational part which is that of a "displaced oscillator."[20] But as the couplings are different for the two triplets, the displacements for the oscillators will be different. An estimate of the coupling coefficients with the Γ_{3g} modes based on the point-charge model leads to the result

$$V_3(\Gamma_{5g})/V_3(\Gamma_{4g}) \sim -0.7 \ .$$

Owing to the sign of this ratio, the potential wells associated with the Γ_{5g} states are on the vertices of an equilateral triangle which has a different orientation than that of the equilateral triangle of the potential wells associated with the Γ_{4g} ground state. Matrix elements of spin-orbit coupling between ground and excited vibronic levels are of the form

$$\langle m_s ;\ \Gamma_{4g}, i ;\ i\,00 \,|\, \lambda(\vec{L}\cdot\vec{S}) \,|\, m_s' ;\ \Gamma_{5g},\ \alpha ;\ \alpha n m \rangle \ ,$$

where the spin, the electronic, and the vibrational parts of the states are explicitly written. A general term of second order is then

$$\sum_{\substack{m_S'',\alpha \\ n,m}} \frac{\langle m_S ; i ; i\,00 \,|\, \lambda(\vec{L}\cdot\vec{S}) \,|\, m_S'' ;\ \alpha ;\ \alpha n m\rangle \langle m_S'' ;\ \alpha ;\ \alpha n m \,|\, \lambda(\vec{L}\cdot\vec{S}) \,|\, m_S' ;\ j ;\ j\,00\rangle}{\Delta + (n+m)\hbar\omega} \ .$$

These terms are similar to those considered by Ham[20] for the second-order vibronic effects, but here the denominator has the additional quantity Δ and the states with $n = m = 0$ are included. Then $\Delta \gg (n+m)\hbar\omega$ even for moderately large values of $(n+m)\hbar\omega$. For higher values of $(n+m)$, the overlap integral of the corresponding vibrational states with the ground vibrational states become very small. We thus can drop the term $(n+m)\hbar\omega$ in the denominator. Then, using the closure relation

$$\sum_{n,m} |\, \alpha n m \rangle \langle \alpha n m \,| = 1 \ ,$$

we obtain

$$\frac{\lambda_f^2}{\Delta} \Big[\sum_{\alpha, m_S''} \langle m_S, i \,|\, (\vec{L}\cdot\vec{S}) \,|\, m_S'', \alpha \rangle \langle m_S'', \alpha \,|\, (\vec{L}\cdot\vec{S}) \,|\, m_S', j \rangle \Big] \langle i\,00 \,|\, j\,00 \rangle \ .$$

We note that the term in brackets is the term we obtained in the calculation where the Jahn-Teller interaction was ignored. Thus, this equation shows that only the off-diagonal matrix elements are reduced, and furthermore with the same reduction factor as for the first-order term,

$$K(\Gamma_{4g}) = \langle i\,00 \,|\, j\,00 \rangle = e^{-3E_{JT}/2\hbar\omega} \quad (i \neq j) \ .$$

This results in a reduction for the splitting D' given by (15) to the value

$$D_r' = \tfrac{1}{2}(1 + e^{-3E_{JT}/2\hbar\omega}) D' \ . \qquad (16)$$

Finally, we have obtained a third value of the splitting by a calculation in which term mixing is included but Jahn-Teller coupling ignored. This calculation is easily made with the help of the matrix elements of spin-orbit coupling given by Liehr and Ballhausen in their paper on the d^2 configuration in a cubic crystal field.[21] We do not give the analytical result of this calculation because the value obtained, denoted by D'', is only slightly different from D' when we substitute numerical values (see below). We shall suppose that the reduction of D'' by the Jahn-Teller effect is the same as that of D' as given by (16).

B. g Factor

As in the absence of a Jahn-Teller interaction the electronic excited levels have no effect on the g value, the calculations are simpler than for the splitting. Ham[20] has calculated the Zeeman effect including the second-order contribution due to vibronic levels. He obtains a first-order effective Hamiltonian

$$\mathcal{H}_z^{(1)} = g_{\mathcal{L}}\, \mu_B (\vec{H}\cdot\vec{\mathcal{L}}) + 2\mu_B (\vec{H}\cdot\vec{S})$$

and a second-order effective Hamiltonian

$$\mathcal{H}_z^{(2)} = g_1 \mu_B [(\vec{H}\cdot\vec{\mathcal{L}})(\vec{\mathcal{L}}\cdot\vec{S}) + (\vec{\mathcal{L}}\cdot\vec{S})(\vec{H}\cdot\vec{\mathcal{L}})] + g_2 \mu_B (\mathcal{L}_x^2 S_x H_x + \mathcal{L}_y^2 S_y H_y + \mathcal{L}_z^2 S_z H_z) \ ,$$

with

$$g_{\mathcal{L}} = c\, g_L\, K(\Gamma_{4g}) \ ,$$

$$g_1 = -\frac{\lambda_f g_L^2 c^2}{\hbar\omega} \exp\left(-3\frac{E_{JT}}{\hbar\omega}\right) G\left(\frac{3}{2}\frac{E_{JT}}{\hbar\omega}\right) \ ,$$

$$g_2 = -\frac{2\lambda_f g_L^2 c^2}{\hbar\omega} \exp\left(-3\frac{E_{JT}}{\hbar\omega}\right) G\left(3\frac{E_{JT}}{\hbar\omega}\right) \ .$$

When applied to our case, these Hamiltonians lead to the following g value for the triplet in which the resonance is observed:

$$g = 1 + \tfrac{1}{2} c g_L K(\Gamma_{4g}) + g_1 \ .$$

C. Comparison with Experimental Results and Discussion

For this comparison, we must estimate the splitting Δ induced by the cubic crystal field. This can be made from optical measurements of Sturge[22] who has attributed the two lines observed at 16 000 and 22 200 cm^{-1} to the transitions $|{}^3F, \Gamma_{4g}\rangle \rightarrow |{}^3F, \Gamma_{5g}\rangle$ and $|{}^3F, \Gamma_{4g}\rangle \rightarrow |{}^3P, \Gamma_{4g}\rangle$. We thus obtain

$$\Delta = 16\,000 \text{ cm}^{-1}, \quad \tan 2\alpha = 0.28 \ , \quad g_L = -1.24 \ .$$

The splittings D' and D'' are, taking into account covalency,

$$D' = 4.7 c^2 \lambda_f^2 \times 10^{-4} \text{ cm}^{-1} \ ,$$

$$D'' = 4.3 c^2 \lambda_f^2 \times 10^{-4} \text{ cm}^{-1} \ .$$

They are reduced as indicated by Eq. (16). We must then determine the values of c, $x = 3E_{JT}/\hbar\omega$, and $\hbar\omega$ which best fit the two equations:

$$D_{\text{expt}} = D''\left[\tfrac{1}{2}(1 + e^{-x/2})\right] + (\lambda_f^2 g_L^2 c^2/\hbar\omega) e^{-x} \left[G(x) - G(\tfrac{1}{2}x)\right] \ ,$$

$$g_{\text{expt}} = 1 + \tfrac{1}{2} c g_L e^{-x/2} - (\lambda_f g_L^2 c^2/\hbar\omega) e^{-x} G(\tfrac{1}{2}x) \ ,$$

with $D_{\text{expt}} = 7$ cm^{-1}, $g_{\text{expt}} = 0.67$,[11] and $\lambda_f = 104$ cm^{-1}. From the work of Sangster and McCombie[23] on vibrational structure of the optical lines of ions in MgO, we choose $\hbar\omega = 450$ cm^{-1}. The best values for the fitting are $c = 0.72$ and $x = 0.9$. We deduce

$$K(\Gamma_{4g}) = 0.64 \text{ and } E_{JT} = 135 \text{ cm}^{-1} \ .$$

Although these values are not precise, they show that V^{3+} in MgO is a weakly coupled Jahn-Teller system. The small difference between the Jahn-Teller energy and the spin-orbit interaction seems to invalidate the perturbation-theory calculation. We can point out, however, that this calculation is justified *a posteriori* since the spin-orbit coupling is reduced by the Jahn-Teller effect. Had the spin-orbit coupling been slightly weaker, it would have stabilized the Jahn-Teller interaction. As a consequence, the second-order effects are important, as seen above.

We can deduce the value of V_3, the coupling coefficient between the ion and the vibrational modes of the cluster XY_6, using the equation $E_{JT} = V_3^2/2\mu\omega^2$, where μ is the mass of the Y ions of the cluster.[20] With the preceding values for E_{JT} and ω, we obtain $V_3 = 10^{-4}$ erg/cm. We can also deduce the coupling coefficient V_3' between the ion and the strains or the long-wavelength vibrational modes by noting that $V_3' = (\sqrt{3}/R) G_{11}$, R being the X-Y distance. With the value of $G_{11} = 1500$ cm^{-1}, we deduce $V_3' = 2.4 \times 10^{-5}$ erg/cm. We also calculate a theoretical value V_3'' from the usual point-charge model,

$$V_3'' = \frac{\sqrt{3} Z_{\text{eff}} e^2}{7R^4} \left(-\frac{12}{5} \langle r^2 \rangle + \frac{25}{6} \frac{\langle r^4 \rangle}{R^2} \right) .$$

Taking $Z_{\text{eff}} = 2$, $\langle r^2 \rangle = 1.64 a_0^2$, $\langle r^4 \rangle = 5.45 a_0^4$ [24] (where a_0 is the Bohr radius), we have $V_3'' = 4 \times 10^{-5}$ erg/cm. In view of the various approximations made to obtain *each* of these values, we think it is impossible to make a meaningful comparison. We can only remark that they are of the same order of magnitude.

V. CONCLUSION

We have developed a method which permits the calculation of the influence of the random strains in cases where their effect is of the same order of magnitude as the Zeeman effect. The application of that method to the system V^{3+}:MgO has led to theoretical spectra which are in good agreement with the experiments. The method has the advantage of not masking the physics involved behind the numerical calculations. It permits us, for instance, to look at the nature of the distortion of the ions which contribute to a definite part of the spectrum. The important result is the explanation of the existence of an *anisotropic* spectrum due to ions which are in *cubic* sites on the average. In other words, we have explained this anisotropic spectrum using a Gaussian distribution centered around zero strain as we had recently proposed.[11] We have also deduced, from a fitting of theoretical and experimental spectra, the value of the ion-strain coupling. This value, as the Jahn-Teller energy value deduced from the characteristics of the APR spectrum, shows that the V^{3+} ion in MgO is a weakly coupled system where the vibronic second-order effects are important. It is indicated also that this system is near the region where the spin-orbit interaction reduces the Jahn-Teller effect instead of being reduced by it. It will be of interest to compare this system with the CaO:V^{3+} system on which experiments are in progress.

Note added in proof. It is perhaps helpful to add some comments in order to better illustrate this work and to compare it with the work of Ham.[9] He has shown, for another system and in the case where the effect of strains is large ($\delta \gg 1$ in our notation), that ions which are in nearly tetragonal symmetry have their resonance at the same value of the magnetic field, whatever the strength of the tetragonal distortion. Thus, only these ions can give observable lines, a result which we have also obtained with our method (see Figs. 7 and 8). The interesting point is that even in the case $\delta \sim 1$, the behavior is qualitatively

the same, as shown in Figs. 4 and 5. Though the spectrum is more complex, it contains peaks whose position approximately follows the $1/\cos\theta$ tetragonal relation. However, Fig. 10 shows that the relative contribution to the observed spectrum of these particular ions becomes more and more reduced as δ decreases. The hypothesis of a distribution centered around zero for the random strains has also been made by Ray. The difference between her recent work [T. Ray, Phys. Rev. B 5, 1758 (1972)] and ours lies only in the fact that we give proof that such a distribution leads to tetragonal peaks while she has not considered the angular dependence of the spectrum.

ACKNOWLEDGMENTS

It is a pleasure for the authors to thank Professor P. J. Laurent for his help for the procedure of generation of random numbers, Dr. Y. Merle D'Aubigné and R. Romestain for very fruitful discussions, and Miss Nedelka and M. Merlin for help in the programming.

APPENDIX A: THEORETICAL LINE SHAPE

With the reduced values defined by Eqs. (4), the magnetic field is represented by λ and the energy of the transition by unity. If we denote the line shape by $I(\lambda)$, the part of the line within λ and $\lambda+d\lambda$ is due to ions which have two levels separated by unity when λ is in this interval. Thus, $I(\lambda)d\lambda$ = [probability of finding two levels such that $\Delta E=1$, when λ is in the interval $(\lambda,\ \lambda+d\lambda)$]$\times$[transition probability for the corresponding transition].

Let E_i and $|i\rangle$ be the eigenvalues and eigenvectors of Hamiltonian (3). The resonance condition for the levels i and j is $|E_i-E_j|-1=0$, which we denote as $g(i,j,X,Y,\lambda)=0$. In the XY plane, this condition defines a curve C_λ. If λ takes the value $\lambda+d\lambda$, the corresponding curve is $C_{\lambda+d\lambda}$ and its equation is $g(i,j,X,Y,\lambda+d\lambda)=0$. Let D_{ij} be the part of the XY plane which is contained between these curves, and $p(X,Y)$ be the distribution function for the random variables X and Y. Then

$$I(\lambda)d\lambda=\sum_{i,j}\int\int_{D_{ij}}p(X,Y)dXdY\,|\langle i|\mathcal{H}_1|j\rangle|^2$$

$$=\sum_{i,j}\int\int_{D_{ij}}F(i,j,X,Y)dXdY\ ,$$

where $\mathcal{H}_1$ is the Hamiltonian (7) or (8). For the evaluation of this integral we can write, as usual,

$$I(\lambda)d\lambda=\sum_{i,j}\int_{X_1(i,j)}^{X_2(i,j)}dX\int_{Y_1(i,j,X)}^{Y_2(i,j,X)}dYF(X,Y)\ ,$$

where the limits of integration are specific of each domain D_{ij}. For the integration over Y, the value of X is fixed. Thus, $Y_1(i,j,X)$ is a root of $g(i,j,X,Y,\lambda)=0$ and $Y_2(i,j,X)$ is a root of $g(i,j,X,Y,\lambda+d\lambda)=0$. If we denote $Y_2=Y_1+\Delta Y$, we obtain $\Delta Y=-d\lambda\,(g'_\lambda/g'_Y)_{(Y_1)}$, and thus

$$I(\lambda)=-\sum_{i,j}\int_{X_1(i,j)}^{X_2(i,j)}dXF[X,Y_1(X)](g'_\lambda/g'_Y)_{(Y_1)}\ . \tag{A1}$$

APPENDIX B: GENERATION OF GAUSSIAN RANDOM NUMBERS

The following procedure was indicated by Laurent of the Mathematics Department.

If U is a random variable uniformly distributed in the interval $[0,1]$, $V=-\ln U$ is a positive random variable having e^{-v} as a distribution function. Let us consider the function $g(V,W)=e^{-(1-V)^2/2}-W$, where W is another random variable uniformly distributed in $[0,1]$. As $e^{-(1-V)^2/2}\leq 1$, the probability for $g(V,W)$ to have a value in $[0,1]$ when $V=v$ is simply $e^{-(1-v)^2/2}$. Among the possible values for V, we call R those which are such that $g(V,W)$ is in the interval $[0,1]$. The distribution function for R is the product $e^{-v}e^{-(1-v)^2/2}=(1/\sqrt{e})e^{-v^2/2}$, i.e., a Gaussian function of unity half-width.

The generation of random variables uniformly distributed in $[0,1]$ was made using an internal algorithm of the IBM 360-65 computer. Taking two such variables U and W, we calculate $V=\ln U$ and we retain only the values of V such that $-\ln W\geq\frac{1}{2}(1-V)^2$. These are the R numbers and they are positive. To get a symmetrical distribution function, we use another variable uniformly distributed in $[0,1]$. When it is greater than $\frac{1}{2}$, we take the number R; when it is less than $\frac{1}{2}$, we take the number $-R$.

---

*Laboratoire associé au CNRS.

[1]D. H. McMahon, Phys. Rev. 134, A128 (1964).

[2]E. R. Feher, Phys. Rev. 136, A145 (1964).

[3]P. Donoho, Phys. Rev. B 3, 645 (1971).

[4]A. M. Stoneham, Rev. Mod. Phys. 41, 82 (1969).

[5]J. R. Herrington, T. L. Estle, and L. A. Boatner, Phys. Rev. B 3, 2933 (1971).

[6]U. T. Hochli, Phys. Rev. 162, 262 (1967).

[7]F. S. Ham, Phys. Rev. 166, 307 (1968).

[8]J. R. Fletcher and K. W. H. Stevens, J. Phys. C 2, 444 (1969).

[9]F. S. Ham, Phys. Rev. B 4, 3854 (1971).

[10]R. Buisson and C. Jacolin, J. Phys. (Paris) 30, 103 (1969).

[11]R. Buisson and A. Nahmani, Phys. Letters 37A, 9 (1971).

[12]T. Ray, Solid State Commun. 9, 911 (1971).

[13]J. S. Griffith, *The Theory of Transition Metal Ions* (Cambridge U. P., Cambridge, England, 1961).

[14]M. Borg, R. Buisson, and C. Jacolin, Phys. Rev. B 1, 1917 (1970).

[15]The result given in Ref. 10 is erroneous, but it is only slightly different from the correct result, and the conclusions of this paper remain valid.

[16]A. Abragam and B. Bleaney, *E. P. R. of Transition Ions* (Clarendon, Oxford, England, 1970).

[17]F. G. Marshall and V. W. Rampton, J. Phys. C 1, 594 (1968).

[18]R. G. Brabin-Smith and V. W. Rampton, J. Phys. C 2, 1759 (1969).

[19]C. A. Bates, L. C. Goodfellow, and K. W. H. Stevens, J. Phys. C 3, 1831 (1970).

[20]F. S. Ham, Phys. Rev. 138, A1727 (1965).

[21]A. D. Liehr and C. J. Ballhausen, Ann. Phys. (N.Y.) 2, 134 (1959).

[22]M. D. Sturge, Phys. Rev. 130, 639 (1963).

[23]M. J. L. Sangster and C. W. McCombie, J. Phys. C 3, 1498 (1970).

[24]E. B. Tucker, Phys. Rev. 143, 264 (1966).